

## Evaluation of Carbon Fiber distribution in Unidirectional CF/Al Composites by Two-Dimensional Spatial Distribution Method

Moonhee Lee<sup>1\*</sup>, Sungwon Kim<sup>1</sup>, Jongho Lee<sup>1</sup>, SeungKuk Hwang<sup>2</sup>, Sangpill Lee<sup>3</sup>, Kenjiro Sugio<sup>4</sup>, Gen Sasaki<sup>4</sup>

### 〈Abstract〉

Low pressure casting process for unidirectional carbon fiber reinforced aluminum (UD-CF/Al) composites which is an infiltration route of molten Al into porous UD-CF preform has been a cost-effective way to obtain metal matrix composites (MMCs) but, easy to cause non-uniform fiber distribution as CF clustering. Such clustered CFs have been a problem to decrease the density and thermal conductivity (TC) of composites, due to the existence of pores in the clustered area. To obtain high thermal performance composites for heat-sink application, the relationship between fiber distribution and porosity has to be clearly investigated. In this study, the CF distribution was evaluated with quantification approach by using two-dimensional spatial distribution method as local number 2-dimension (LN2D) analysis. Note that the CFs distribution in composites sensitively changed by sizes of Cu bridging particles between the CFs added in the UD-CF preform fabrication stage, and influenced on only LN2D<sub>var</sub> values.

*Keywords : CF/Al composites, low pressure infiltration, fiber distribution, computerexperiment*

---

1\* Corresponding Author, Division of Mechanical Engineering, Dong-Eui Institute of Technology, Ph.D(Eng.)  
E-mail : mhlee81@dit.ac.kr

1 Division of Mechanical Engineering, Dong-Eui Institute of Technology, Busan, 47230, Republic of Korea

2 Computer Aided Mechanics Department, Changwon Campus Korea Polytechnic, 51519, Republic of Korea

3 Department of Mechanical Engineering, Dong-Eui University, Busan, 47340, Republic of Korea

4 Materials and Production Engineering, Institute of Engineering, Hiroshima University, Higashi-Hiroshima 739-8527, Japan

## 1. Introduction

The high performance thermal packaging materials have been developed to prevent the performance degradation of the electric or electronic components from their inevitable heat generation[1-3]. Especially, recently developing high-performance and high-integrated optical components or power devices such as light-emitting diode (LED) modules and insulated-gate bipolar transistor (IGBT) modules[4-6] which are considered to apply to automobile or portable devices have been required higher thermal conductivity (TC) and lower coefficient of thermal expansion (CTE) heat-sink materials, replaceable to conventional ones.

For the heat-sink materials, metal matrix composites (MMCs) have been noticeable with their own advantages as tailorable TC and CTE, simple fabrication process and low cost [7-9]. Recently developed coal-tar pitch based unidirectional carbon fibers (UD-CFs) as reinforcements for MMCs exhibits very high TC of  $800 \text{ Wm}^{-1}\text{K}^{-1}$  with extremely low CTE of below  $5.0 \times 10^{-6} \text{ K}^{-1}$  in longitudinal direction to the unidirectional fiber axis. Al matrix composites reinforced with those UD-CFs, in particular, are expected to accomplish as-mentioned requirements for weight-saving heat-sink.

The Al matrix composites typically fabricated by high pressure casting process. High pressure fabrication system for MMCs always causes not only high cost but also

size and shape limitation. On the other hands, the low pressure casting for MMCs called low pressure infiltration (LPI) process[10, 11] enables complex/large shape, simple apparatus and cost-saving fabrication. The LPI process for fiber reinforced MMCs are carried out by infiltration of molten metal into a porous fiber preform with low applied pressure. However, it is difficult to maintain uniform fiber array in the preform. In the previous study, Cu particles were dispersed between CFs as a fiber-bridging material and then sintered by spark plasma sintering (SPS) to obtain UD-CF preform with homogeneous CF arrays[12, 13]. It also reported that the size variation of Cu particles affected to the homogeneity of fiber array distribution and the densification of the composites. That is, the different Cu sizes seemed to change the degree of local inhomogeneous distribution of UD-CFs to some extent. Such inhomogeneous distribution can lead to fiber clustering and further internal pores by imperfect infiltration of molten Al in those clustered region during LPI process. The pores are expected to degrade TC of the composites to some extent by disturbing heat flow in Al matrix and matrix-fiber interfaces. However, the effect of qualitative and/or quantitative approach for fiber distribution changing porosity has not been verified.

Recently spatial distribution descriptors such as 2-dimensional local number (LN2D) or 3-dimensional local number (LN3D) method have been used to estimate the

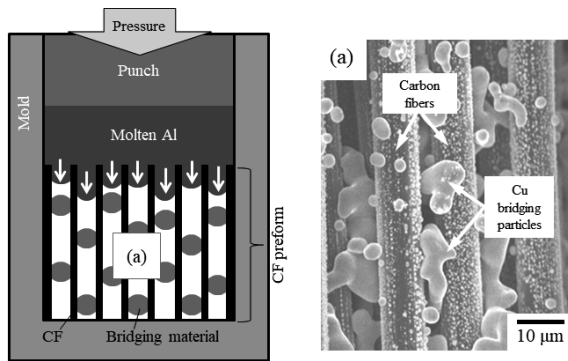


Fig. 1 Illustration of low pressure infiltration (LPI) method infiltrating molten Al into (a) porous CFs preform for unidirectional CF/Al composites

Table 1. Cu particle size dependence on density of unidirectional CF/Al composites [12]

CF preform	CF volume (%)	30			
	Cu volume (%)	10			
	CF size ( $\mu\text{m}$ )	11			
	Cu size ( $\mu\text{m}$ )	2.55	28.86	11.79	2.55+11.79
CF/Al composites	Relative density (%)	1.88	2.09	2.86	3.00

spatial distribution of second-phase particles in MMCs by quantitative experiment[14-16]. In case of the distribution of UD-CFs in Al matrix, the LN2D evaluation from the cross-sectional microstructure of UD-CFs in UD-CF/Al composites can be useful method.

In this study, the distribution of UD-CFs in UD-CF/Al composites depending on added Cu sizes was evaluated by the quantitative analysis using LN2D method. Moreover, the

relationship between fiber distribution values and porosity of the composites was also discussed.

## 2. Procedure of Experiments

### 2.1 Preparation of UD-CF/Al composites

The coal tar pitch based UD-CFs (K13D2U, Mitsubishi Plastics, Inc.) in  $11\ \mu\text{m}$  diameter and Cu particles with four different average particle sizes ranged from 2.55 to  $28.86\ \mu\text{m}$  (Fukuda metal, foil & powder Co, LTD) were prepared as raw materials for UD-CF preforms. The UD-CF preforms were fabricated by SPS process as follows: The Cu particles mixed with polyethylene-glycol (PEG) as dispersant were dispersed in UD-CF bundles by rolling process. Subsequently, the UD-CF mixtures were put into the graphite mold in dimension of  $\varnothing 10 \times H10\ \text{mm}^3$  and spark sintered [13]. The spark sintering conditions to obtain porous CF preforms from CF-Cu mixtures were the sintering temperature of 1123 K for 1800 s with the constant electrical voltage and current of 4 V and 390 A under vacuum of  $2.7 \times 10^{-2}\ \text{Pa}$  without applied pressure. The volume of UD-CFs and Cu particles in CF preform was 0.3 and 0.1, respectively. The LPI process was carried out on those obtained porous preforms for the fabrication of UD-CF/Al composites, as shown in Fig. 1: The porous

UD-CF preform was set into the graphite mold with vertical directional arrangement of UD-CFs array and the molten Al (A1070) poured into the upper part of the preform and then pressed by graphite punch. The molten Al was infiltrated into vacant inter-fiber regions of the UD-CF preform at 1123 K for 60 s with the external applied pressure of 0.8 MPa under Ar environment. The microstructures of obtained UD-CF/Al composites were observed by scanning electron microscopy (SEM). Fig. 2 represents the cross-sectional SEM images of UD-CF/Al composites added with different Cu particle sizes. Those microstructures exhibit somewhat different distribution of CFs depending on the size of added Cu particles. Such difference affect to density of the composites significantly, as shown in Table 1.

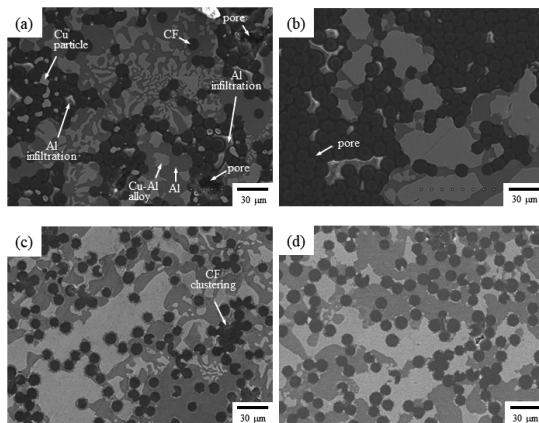


Fig. 2 Cross-section SEM images of unidirectional CF/Al composites added with Cu bridging particle sizes of (a) 2.55  $\mu\text{m}$  [12], (b) 28.86  $\mu\text{m}$  [12], (c) 11.79  $\mu\text{m}$  and (d) bimodal (mixed with 2.55 and 11.79  $\mu\text{m}$ )

## 2.2 Definition and measurement of LN2D

The differences of CFs distribution were clarified by LN2D method. It can be assumed that the gravity centers (GCs) of cross-sectional circle shapes of UD-CFs are arranged in homogeneous distribution such as closest hexagonal structure. In this case, one GC is surrounded by closest other GCs of neighboring CFs.

Previous studies [14-16] defined a circle named ‘measuring circle’ having a center at a GC of a dispersed particle, and the radius ( $R_{2D}$ ) of the measuring circle determined by the distance between closest other GCs and the GC at the center of measuring circle. The definition of measuring circles was also applied at the cross-sectional microstructure of UD-CF/Al composites in this study.

In the ‘closed-packed’ hexagonal structure of CFs in Al matrix, namely ‘ordered distribution’, as shown in Fig. 3, one measuring circle includes 7 GCs and the number density per unit area is determined to  $7/\pi R_{2D}^2$ . Since the local number density can be regarded as the whole number density,  $\lambda_A$  and  $R_{2D}$  can be expressed as follows[14-16] ;

$$\frac{7}{\pi R_{2D}^2} = \lambda_A \rightarrow R_{2D} = \left( \frac{7}{\pi \lambda_A} \right)^{1/2} = \frac{1.493}{\lambda_A^{1/2}} \quad (1)$$

Note that the number of GCs in the measuring circle is defined as LN2D. Since

the ordered distribution has unique frequency average ( $LN2D_{ave}$ ) and variance ( $LN2D_{var}$ ) values, the values of random or disordered distribution can be easily evaluated the quantitative difference of distribution comparing to the ordered distribution.

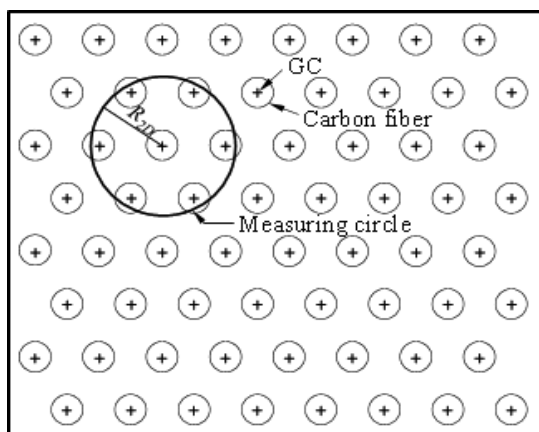


Fig. 3 Example of ordered distribution of CFs in the cross-section of unidirectional CF/Al composites

In this study, the conditions of measurement and experimental domain were followed previous study [16] to eliminate errors. In order to obtain relative frequency distributions of LN2D,  $1.0 \times 10^6$  data of LN2D were collected for each fabrication condition of UD-CF/Al composites.

### 3. Results and Discussion

Various CFs distribution types of UD-CF/Al composites depending on added Cu particle

sizes of each 2.55, 2.55+11.79, 11.79 and 28.86  $\mu\text{m}$  are shown in Fig. 2. It was revealed that the added Cu sizes affected not only CFs distribution but also density of the composites in the previous study [12]. The theoretical Cu spacer sizes were calculated by geometrical models based on a reference [17] for uniform fiber arrays, and thus the theoretical Cu sizes for 30 vol% of 11  $\mu\text{m}$  diameter CFs were calculated to 11.08 and 14.17  $\mu\text{m}$  for uniform square and hexagonal CFs distribution, respectively [12]. The addition of Cu particles with near theoretical size (11.79  $\mu\text{m}$ ) in UD-CF/Al composites in Fig. 2 (c) showed less CFs clustering and higher density than that of small size (2.55  $\mu\text{m}$ ) or large size (28.86  $\mu\text{m}$ ) in Fig. 2 (a) and (b). The composites added 2.55+11.79  $\mu\text{m}$  Cu to eliminate even still remained CF cluster in Fig. 2 (c) showed near-fully dense morphology without significant CF clustering in Fig. 2 (d). According to the result of measured density for each composite in Table 1, the size control of Cu particles revealed an effective way to avoid fiber clustering in the composites remarkably.

Fig. 4 exhibits measured LN2D results of CF distribution in UD-CF/Al composites depending on added Cu sizes. The calculated relative frequency of LN2D for close-packed structure model are compared with the measured results. Their 'average' and 'variance' results of LN2D are listed in Table 2. The LN2D results on the close-packed structure model showed a sharp peak with

the frequency average,  $LN2D_{ave}$  of 7.00462 and extremely narrow frequency variance  $LN2D_{var}$  of 0.340141. Note that if the measured  $LN2D_{ave}$  and  $LN2D_{var}$  of random CFs distribution in the composites are as close as the results of close-packed structure model, the distribution tends toward homogeneous. From the measured results on the composites, the ' $LN2D_{ave}$ ' did not have any distinguishable differences regardless of added Cu sizes even comparing to the close-packed structure model. However, the ' $LN2D_{var}$ ' of those results exhibited decisive difference. The composite added with 28.86  $\mu\text{m}$  Cu particles, in particular, has the large difference of  $LN2D_{var}$  comparing to that of close-packed structure model. The composite also showed the widely-scattered  $LN2D$  frequency by relatively high frequency at the range below 5 or above 10, comparing to the other measured results, as shown in Fig. 4. Those  $LN2D$  results are obviously caused by the wide local fiber clustering region and the adjacent wide matrix region containing few fibers in Fig. 2 (b). Such polarization of CF distribution leading to density decrease of the composite was caused by insufficient infiltration of molten Al into clustered fibers of UD-CF preform. It meant that adding unsuitable Cu size in UD-CF preform affected  $LN2D_{var}$  with fiber clustering in the composite.

Except of the composites added with 28.86  $\mu\text{m}$  Cu particles, all of the composites exhibited concentrated  $LN2D$  frequency

around 7. Of course, two composites added with each 2.55 and 11.79  $\mu\text{m}$  Cu particles of did not show big distinction on  $LN2D_{var}$ , but their porosities were significantly different. Indeed, the composite added with 11.79  $\mu\text{m}$  Cu showed low porosity of about 10 %, whereas the porosity of the composite added with 2.55  $\mu\text{m}$  Cu was higher than even the composite added with 28.86  $\mu\text{m}$  Cu. Small Cu spacing in the fiber clustering region, as shown in Fig. 2 (a), is expected to lower the  $LN2D_{var}$  values of the composite. However, those spaces did not have enough area to infiltrate molten Al because of poor-wettability between carbon and molten Al. That is, the delicate difference of  $LN2D_{var}$  between the composites added with each 2.55 and 11.79  $\mu\text{m}$  Cu particles can be sensitive turning-point whether having adequate fiber spacing for molten Al

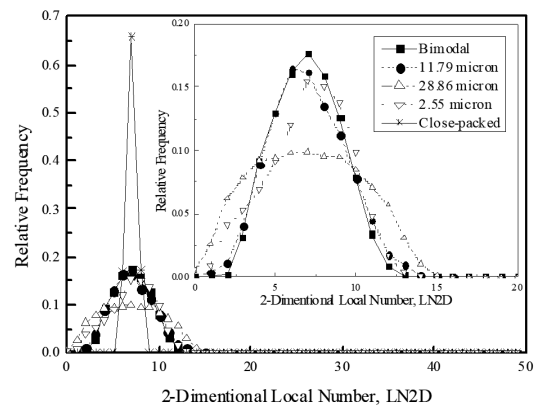


Fig. 4 Relative frequency of calculated  $LN2D$  for CF distribution in unidirectional CF/Al composites added different sizes of fiber-bridging Cu particles, comparing with the closed-packed distribution structure

Table 2. Frequency average and variance of LN2D of CF distribution in unidirectional CF/Al composites

Close-packed model		LN2D <sub>av</sub>	LN2D <sub>var</sub>	Porosity of composites (%)
		7.00462	0.3401	
CF distribution with fiber bridging particles	2.55 $\mu$ m Cu	7.00248	6.5377	41
	28.86 $\mu$ m Cu	7.0037	10.831	34
	11.79 $\mu$ m Cu	7.00127	5.4179	10
	2.55 + 11.79 $\mu$ m Cu	7.00045	4.2612	5

infiltration or having insufficient fiber spacing as clustering which causes imperfect infiltration easily. Moreover, the addition of 11.79  $\mu$  m Cu particles demonstrated effective to uniform fiber distribution in this study. In other words, the UD-CF/Al composites with LN2D<sub>var</sub> below 5.4 exhibits high density restraining detrimental fiber clustering when the fiber volume fraction is 0.3. The composite added bimodal size of Cu particles showing lowest LN2D<sub>var</sub> of 4.2612 exhibited lowest porosity of 5 % and extremely rare fiber clustering. From these results, LN2D analysis from the cross-sectional SEM images can be a simple and effective way for the quantification of fiber distribution contributing to the densification of UD-CF/Al composites. It is expected that such LN2D analysis for fiber distribution can be widely applied on the optimization of fabrication conditions for high performance MMCs.

#### 4. Conclusions

In this study, the relationship between CFs distribution and densification of UD-CF/Al

composites fabricated LPI process has been investigated with LN2D analysis, density and microstructure observation for high performance heat-sink MMCs. Especially, the size variation of Cu particles, which were added at the stage of CF preform fabrication for CFs bridging influenced on the LN2D<sub>var</sub> values of CFs distribution and density of UD-CF/Al composites. The widely scattered LN2D frequency data and high LN2D<sub>var</sub> value of the composites added with large Cu size of 28.86  $\mu$  m exhibited poor density with significant and harsh fiber clustering. Meanwhile, other composites added 2.55, 11.79  $\mu$  m and bimodal Cu led to concentrated peak of LN2D frequency data toward 7 and low LN2D<sub>var</sub> value with decreasing fiber clustering. The delicate difference of LN2D<sub>var</sub> but significant difference of porosity on the composites added each 2.55 and 11.79  $\mu$  m Cu were related whether sufficient or insufficient fiber spacing for Al infiltration. The composites added bimodal Cu size exhibited the lowest LN2D<sub>var</sub> with high densification. Although these results are intended for particular cases only when the diameter and volume fraction of CF were 11

$\mu\text{m}$  and 0.3 in UD-CF/Al composites, the LN2D analysis can be expanded for the quantitative approach to evaluate the distribution of reinforcements in MMCs.

### Acknowledgement

This paper was supported by 2017 Academic Research Grant of Dong-Eui Institute of Technology, Republic of Korea.

### References

- [1] C. Zweben: JOM, 44 (1992) 15-23.
- [2] D.D.L. Chung: Appl. Therm. Eng. 21 (2001) 1593-1605.
- [3] J.M. Molina, J. Narciso, L. Weber, A. Mortensen, E. Louis: Mater. Sci. Eng. A 480 (2008) 483-488.
- [4] M. Schöbel, W. Altendorfer, H.P. Degischer, S. Vaucher, T. Buslaps, M. Di Michiel, M. Hofmann: Compos. Sci. and Technol. 71 (2011) 724-733.
- [5] R. Zehring, A. Stuck, T. Lang: Solid-State Electronics 42 (1998) 2139-2151.
- [6] Shan Yin, King Jet Tseng, Jiyun Zhao: Appl. Therm. Eng. 52 (2013) 120-129.
- [7] K. Sugio, Y. Choi, G.Sasaki: Mater. Trans. 57(5) (2016) 582-589.
- [8] J. You: Nuclear Materials and Energy 5 (2015) 7-18.
- [9] O. Lee, M. Lee, Y. Choi, K. Sugio, K. Matsugi, G. Sasaki: Mater. Trans. 55(5) (2014) 827-830.
- [10] Y. B. Choi, G. Sasaki, K. Matsugi, N. Sorida, S. Kondoh, T. Fujii, O. Yanagisawa: JSME A 49 (2006) 20-24.
- [11] Y. B. Choi, K. Matsugi, G. Sasaki, S. Kondoh: Mater. Trans. 49 (2008) 390-392.
- [12] M. Lee, Y. Choi, K. Sugio, K. Matsugi, G. Sasaki: Sci. Eng. Compos. Mater. 18 (2011) 167-171
- [13] M. Lee, Y. Choi, K. Sugio, K. Matsugi, G. Sasaki: Mater. Trans. 52(5) (2011) 939-942.
- [14] G. Sasaki, K. Ishikawa, K. Sugio, Y. Choi, K. Matsugi: The 8th Pacific Rim International Congress on Advanced Materials and Proc. Proceedings (2013) 1487-1492
- [15] K. Sugio, Y. Momota, D. Zhang, H. Fukushima, O. Yanagisawa: Mater. Trans. 48(10) (2007) 2762-2767.
- [16] K. Sugio, Y. Momota, D. Zhang, H. Fukushima, O. Yanagisawa: Mater. Trans. 48(10) (2007) 2768-2777.
- [17] Long S, Zhang Z, Flower HM: Acta Metall. Mater. 42 (1994) 1389-1397.

---

(Manuscript received November 29, 2017; revised December 28, 2017; accepted January 8, 2018.)